

# Rotation-driven prolate-to-oblate shape phase transition in $^{190}\text{W}$ : A projected shell model study<sup>★</sup>

Yang Sun<sup>a,b,c</sup>, Philip M. Walker<sup>d</sup>, Fu-Rong Xu<sup>e,g</sup>,  
Yu-Xin Liu<sup>f,g</sup>

<sup>a</sup>*Institute of Modern Physics, Chinese Academy of Sciences, Lanzhou 730000, P. R. China*

<sup>b</sup>*Department of Physics, Shanghai Jiao Tong University, Shanghai 200240, P. R. China*

<sup>c</sup>*Joint Institute for Nuclear Astrophysics, University of Notre Dame, Notre Dame, IN 46556, USA*

<sup>d</sup>*Department of Physics, University of Surrey, Guildford GU2 7XH, United Kingdom*

<sup>e</sup>*Department of Technical Physics, Peking University, Beijing 100871, P. R. China*

<sup>f</sup>*Department of Physics, Peking University, Beijing 100871, P. R. China*

<sup>g</sup>*Center of Theoretical Nuclear Physics, National Laboratory of Heavy Ion Accelerator, Lanzhou 730000, P. R. China*

---

## Abstract

A shape phase transition is demonstrated to occur in  $^{190}\text{W}$  by applying the Projected Shell Model, which goes beyond the usual mean-field approximation. Rotation alignment of neutrons in the high- $j$ ,  $i_{13/2}$  orbital drives the yrast sequence of the system, changing suddenly from prolate to oblate shape at angular momentum  $10\hbar$ . We propose observables to test the picture.

*Key words:* Prolate and oblate shapes, Shape phase transition, Rotation alignment, Projected Shell Model

*PACS:* 21.10.Re, 21.60.Cs, 27.80.+w

---



---

<sup>★</sup> Dedicated to the memory of Professor Dr. Hans-Jörg Mang.

Understanding the fundamental excitations of many-fermion systems and transitions between different excitation modes is an important issue in mesoscale physics. In nuclei where the ground state is typically a superconducting state with paired nucleons moving in orbits, the low-lying excitation spectrum is generally formed by collective motion (for example, rotation and vibration with different nuclear shapes, or deformation) and nucleon pair breaking. Being a finite-size quantum system, for certain numbers of protons and neutrons, a subtle rearrangement of only a few nucleons among the orbitals near the Fermi surface can result in completely different collective modes, constituting a suitable situation for studying the shape phase transition [1,2,3].

There is evidence for several different types of shape phase transition in nuclei. Casten *et al.* [4] systematically studied spherical-to-deformed ground-state phase transitions as a function of neutron number and proton number; and Regan *et al.* [5] observed the evolution from collective vibrational to rotational structure as a function of angular momentum (see also theoretical discussions [6,7]). What we discuss in this Letter is a robust example of a shape phase transition that occurs along an yrast cascade (the locus of lowest energy states of each spin) between states of prolate and oblate shape in an isolated nucleus.

The neutron-rich Hf and W nuclei with neutron number  $N \approx 116$  are expected to exhibit interesting critical-point phenomena due to competing collectivity of prolate and oblate shapes. Since experimental evidence is sparse, we refer mainly to theoretical predictions (e.g. Refs. [8,9]). In these nuclei, the ground state and low-spin states are of a prolate shape. However, the occupation of low- $K$ ,  $i_{13/2}$  neutron intruder orbits when the shape is oblate favors rotation alignment at moderate spin values. ( $K$  is the symmetry-axis projection of the angular-momentum vector.) This was suggested by energy-surface calculations for  $^{190}\text{W}$  based on a mean-field method [10]. Ref. [10] also suggested that the  $^{190}\text{W}$  structure is a candidate for a classic case of “giant backbending”, of the type originally described by Hilton and Mang [11] in the 1970’s. Confirmation of these suggestions requires additional theoretical investigations as well as experimental data. Here we show, with aid of detailed shell-model-type calculations, that  $^{190}\text{W}$  can exhibit an excellent example of a shape phase transition that differs from the previously known types of phase transition reported in the literature [4,5]. The combination of electrical quadrupole moments or  $B(E2)$  values, and gyromagnetic ratios ( $g$  factors), should be able to give firm confirmation. The isomerism [12,13] is a key feature in giving access to these observables.

Phase transitions in nuclei have been theoretically described mainly by means of algebraic models [6,7,14], in which a transition-driving control parameter appears explicitly in the Hamiltonian. There have been microscopic studies based on mean-field theories (for example, Ref. [15]). Using the Landau theory, Alhassid *et al.* [16] found a universal behavior of rapid changes of the

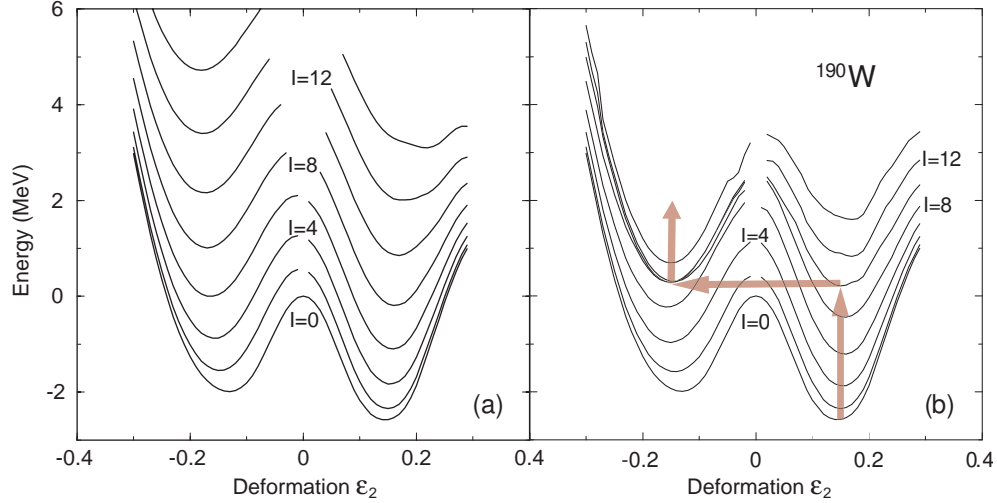


Fig. 1. Energy surface calculation for  $^{190}\text{W}$ . (a) Energies obtained with projection on qp vacuum states only. (b) Energies from calculation with basis that includes 2-qp states.

equilibrium shape from the prolate ground state to oblate excited states in hot rotating nuclei. However, the nuclear shell model can provide a more fundamental basis to study phase transitions. The advantage of a shell-model study is that one may see the microscopic origin of a phase transition by analyzing wave functions. The early work of Federman *et al.* [17] showed perhaps the first example of such a kind. The more recent phase transition study with the Monte Carlo Shell Model [18] and large-scale shell-model calculations [19] are other examples. However, these shell models are applicable only to small nuclear systems, and  $^{190}\text{W}$  is far too large for meaningful calculations of this type.

The Projected Shell Model (PSM) [20] is a shell model that uses deformed bases and the projection technique. It is applicable to any large size of deformed systems (with extreme examples from superdeformed [21] to super-heavy nuclei [22]). The PSM's two-body residual interactions are of the quadrupole plus pairing type, with the quadrupole-pairing term included [20]. Wave functions of the PSM are written in terms of angular-momentum-projected multi-quasiparticle (qp) states

$$|\psi_M^I\rangle = \sum_{\kappa} f_{\kappa}^I \hat{P}_{MK}^I |\phi_{\kappa}\rangle, \quad (1)$$

where the index  $\kappa$  labels basis states.  $\hat{P}_{MK}^I$  is the angular-momentum-projection operator [20] and the coefficients  $f_{\kappa}^I$  are weights of the basis states. For even-even nuclei,  $|\phi_{\kappa}\rangle$  in Eq. (1) is

$$\{|0\rangle, a_{\nu}^{\dagger} a_{\nu}^{\dagger} |0\rangle, a_{\pi}^{\dagger} a_{\pi}^{\dagger} |0\rangle, \dots\} \quad (2)$$

where  $a_\nu^\dagger$  and  $a_\pi^\dagger$  are the creation operator for neutrons and protons, respectively. The qp states are obtained from a deformed Nilsson calculation (with the Nilsson parameters taken from Ref. [23]) followed by a BCS calculation, in a model space with three major shells for each kind of nucleon ( $N = 4, 5, 6$  for neutrons and  $N = 3, 4, 5$  for protons). The corresponding qp vacuum is  $|0\rangle \equiv |\varepsilon\rangle$  at deformation  $\varepsilon$ . We assume axial symmetry in the basis (consistent with Ref. [10]) and, therefore, each basis state in (2) can be labeled by the  $K$  quantum number. While the basis states have good  $K$ , the states of Eq. (1) generally do not, as they are linear combinations of various  $K$ -states.

Fig. 1 shows the projected energy surface calculation for  $^{190}\text{W}$ . The quantities plotted in Fig. 1 are

$$E^I(\varepsilon) = \langle \psi^I(\varepsilon) | \hat{H} | \psi^I(\varepsilon) \rangle. \quad (3)$$

These are energies with different angular momenta  $I = 0, 2, \dots$  calculated as a function of basis deformation  $\varepsilon$ , varying from negative values (corresponding to oblate shapes) to positive values (corresponding to prolate shapes). The energy curves show that there are two pronounced minima, sitting respectively at the prolate and oblate side, with  $|\varepsilon| \approx 0.15$ . The minimum at  $\varepsilon \approx +0.15$  is lower, suggesting that the ground state of  $^{190}\text{W}$  is of prolate shape, which is consistent with the ground state deformation obtained in Refs. [9,10]. The excited  $I = 0$  state, i.e. the minimum at the oblate side with  $\varepsilon \approx -0.15$ , is about 0.6 MeV higher than the ground state. Thus the result predicts a competing picture of prolate and oblate shapes with two sets of corresponding collective states. Dynamic perturbations may change the balance in the competition as the order parameter varies, causing a prolate-to-oblate phase transition.

Perturbations in quantum systems can arise from different sources. The dynamic process responsible for the phase transition in this case is the nuclear rotation and the order parameter is the total spin  $I$ . As the nucleus rotates, individual nucleon pairs tend to align their spins with the collective rotation axis through the Coriolis force. The alignment lowers the system's energy; the amount of energy gain depends primarily on the microscopic structure of the aligned particles. To see this clearly, we compare two calculations in Fig. 1. The left figure shows the calculation in which  $|\psi^I\rangle$  contains the projected qp vacuum state only and all 2-qp states in basis (2) are switched off. The underlying physics is that there is no rotation alignment allowed in the calculation. In such a case, minima on the prolate side remain lower for every state. This implies that the prolate shape always wins in the competition with the oblate shape if no rotation alignment can happen.

Calculations that include 2-qp states in the model space are shown in the right figure in Fig. 1. With inclusion of 2-qp states, energy levels of higher spins are compressed considerably. As the arrows indicate, along the yrast

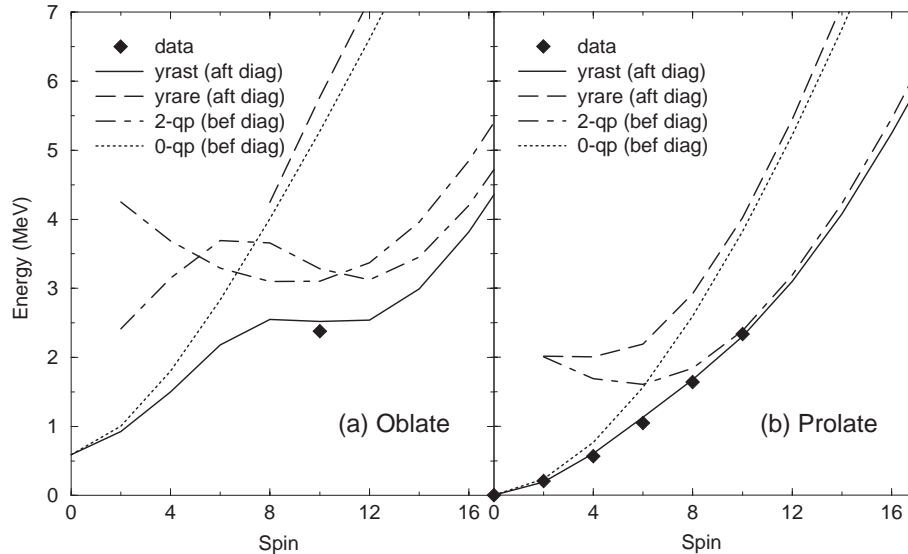


Fig. 2. Selected bands in the  $^{190}\text{W}$  calculation. (a) Bands with oblate shape (calculated at  $\varepsilon = -0.15$ ). (b) Bands with prolate shape (calculated at  $\varepsilon = +0.15$ ).

cascade, the path for the lowest state at each  $I$  starts from the prolate ground state  $I = 0$ , goes up till  $I = 10$ , and then jumps to the oblate side. The wave functions with prolate and oblate shapes are expected to be very different, with a very small overlap between them. Therefore, the above result implies that the yrast cascade of  $\gamma$ -rays is broken and the  $\gamma$  transition between the oblate and prolate states may be strongly hindered. This is a favorable situation for the oblate state at the phase transition to be isomeric. We emphasize that this type of calculation contains beyond-mean-field correlations in the sense that each point in the curves in Fig. 1 is obtained by projecting the intrinsic configurations (deformed mean-field results) onto states with good angular momentum and mixing the projected states through residual interactions.

A phase transition in a quantum many-body system generally refers to an abrupt, qualitative change in the wave function. This subject is of significant interest for many subfields, and is an attractive current topic in nuclear physics [1,2,3]. Our results in Fig. 1 show a clear example of a shape phase transition occurring in an isolated nucleus between two deformed (prolate and oblate) shapes driven by the  $i_{13/2}$  rotation alignment. Coexistence of near-spherical and deformed shapes is a known effect for nuclei near the proton shell closure (see for example  $^{186}\text{Hg}$  [24]). However, the present case with  $N = 116$ , which goes further to the neutron-rich region and has additional valence protons, is more robust. In  $^{186}\text{Hg}$  the ground band is close to spherical and not well developed, but there is also a spin-16 band crossing. This latter feature has parallels with the behavior of  $^{190}\text{W}$ , where the prolate (oblate) wave function contains the highest (lowest)  $K$ -components of the neutron  $i_{13/2}$  orbit (see later discussions), and the wave functions before and after the transition are therefore sharply different.

As long as a nucleus exhibits well-defined deformation minima, such as those shown in Fig. 1, one can apply the PSM and perform detailed shell-model analysis at the minima. To further understand the results in Fig. 1, we show several representative bands in Fig. 2. Angular-momentum-projection on a multi-qp state  $|\phi_\kappa\rangle$  with a sequence of  $I$  generates a band. One may define the rotational energy of a band (band energy) using the expectation values of the Hamiltonian with respect to the projected  $|\phi_\kappa\rangle$  [20]

$$E_\kappa^I = \frac{\langle \phi_\kappa | \hat{H} \hat{P}_{K_\kappa K_\kappa}^I | \phi_\kappa \rangle}{\langle \phi_\kappa | \hat{P}_{K_\kappa K_\kappa}^I | \phi_\kappa \rangle}. \quad (4)$$

These are bands before configuration mixing (diagonal elements in the Hamiltonian matrix) and are denoted as “bef diag” in Fig. 2. Those after configuration mixing, i.e. the superposition of all basis states  $\kappa$  in (1), are denoted as “aft diag”. Bands after mixing are solutions of the eigenvalue problem and dynamics is thus taken into account.

In the calculation for Fig. 2, shell model diagonalization is carried out at two deformations,  $\varepsilon = \pm 0.15$  (see Fig. 1). Note that in the calculation, about 100 2-qp states are included in each diagonalization. We present only a few of them to illustrate the physics. We recall that in  $^{190}\text{W}$ , the neutron occupation is very different at the two energy minima. On the prolate side, one can find high- $K$  orbits such as  $\frac{9}{2}[624]$  and  $\frac{11}{2}[615]$  close to the neutron Fermi surface, while on the oblate side, only the lowest  $K$ -states of the  $i_{13/2}$  intruder shell appear around the Fermi surface. In the right part of Fig. 2, the ground band (dotted curve) starts from the origin and goes up monotonically. At  $I = 6$ , the  $K = 1$ , 2-qp band (dotted-dashed) built by  $\frac{9}{2}[624] \oplus \frac{11}{2}[615]$  quasi-neutrons crosses the ground band. However, interactions at the crossing region are so strong that they repel the crossing bands from each other, forming two smooth sequences. In fact, the resulting bands (solid and dashed curves) are smooth bands as if no band crossing had occurred. The lowest states (solid curve) obtained after configuration mixing reproduce very well the known data (filled diamonds) [13]. On the other hand, in the left part of Fig. 2, the behavior of the low- $K$  2-qp states on the oblate side,  $\frac{1}{2}[660] \oplus \frac{3}{2}[651]$  and  $\frac{1}{2}[660] \oplus \frac{5}{2}[642]$  (both dotted-dashed), is quite different from the 2-qp state on the prolate side. After  $I = 6$ , the combined behavior of these two bands gives rise to nearly degenerate states at  $I = 8, 10$ , and  $12$  lying lowest in energy. These configurations are predicted to be dominant in the lowest oblate states (solid curve), which compares well with the tentative data point from Ref. [13].

One can thus understand that the compression of the states with  $I = 8, 10$ , and  $12$  of the oblate shape is a consequence of the particular rotation-alignment effect of the low- $K$ ,  $i_{13/2}$  neutrons. The effect considerably lowers the total energy, which helps the oblate states to eventually win the prolate-oblate

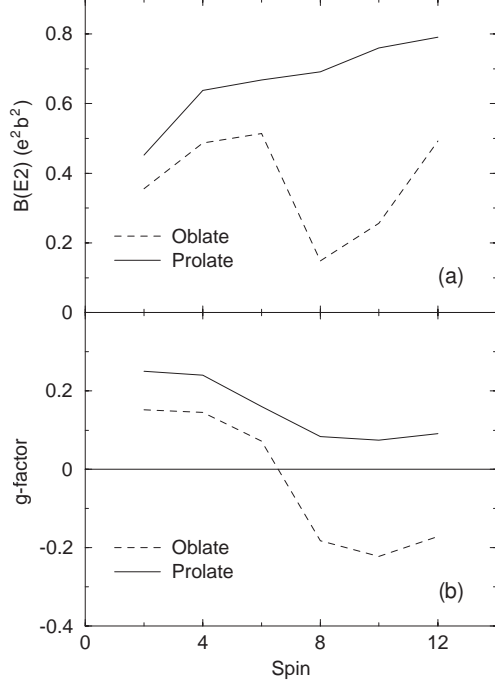


Fig. 3. Predicted electromagnetic properties for  $^{190}\text{W}$ . (a)  $B(E2, I \rightarrow I - 2)$  values. (b)  $g$  factors.

competition. As a result, a prolate-to-oblate shape phase transition occurs along the yrast cascade, and the oblate state with  $I = 10$  becomes isomeric.

Though not shown in Fig. 2, we have found several 2-qp high- $K$  bands with prolate shape in the calculation. The bandhead energies are ranging down to 1.2 MeV of excitation. As some of them lie low in energy and have  $K$ -quantum numbers much differing from the  $K = 0$  ground band, these high- $K$  bands are also predicted to be  $K$ -isomers. The dominant structures of the lowest such bands are:  $K^\pi = 6^+, \frac{3}{2}[512] \oplus \frac{9}{2}[505]$ ;  $K^\pi = 10^+, \frac{9}{2}[624] \oplus \frac{11}{2}[615]$ ;  $K^\pi = 7^-, \frac{3}{2}[512] \oplus \frac{11}{2}[615]$ ; and  $K^\pi = 10^-, \frac{9}{2}[505] \oplus \frac{11}{2}[615]$ .

The energy minimum with oblate shape (see Fig. 1), which lies about 0.6 MeV above the ground state, is a  $0^+$  shape isomer predicted in our calculation. A  $0^+$  shape isomer has been observed in  $^{72}\text{Kr}$  [25]. A recent experiment at GSI may have found evidence [26] for  $\beta$ -decay to this shape isomer.

A crucial test for the above predictions is to measure additional observables for the states before and after the phase transition. As the states belong to very different structures, one may find clear indications when studying their electromagnetic properties, e.g.  $B(E2)$  values and  $g$ -factors.  $B(E2)$  values that are related to the electric quadrupole transition probability from an initial state  $I$  to a final state  $I - 2$  are given by

$$B(E2, I \rightarrow I - 2) = \frac{e^2}{2I + 1} |\langle \psi^{I-2} | \hat{Q}_2 | \psi^I \rangle|^2. \quad (5)$$

The effective charges used in the calculation are the standard ones:  $e_\pi = 1.5e$  and  $e_\nu = 0.5e$ . Magnetic properties are described through  $g$  factors, which are defined as

$$g(I) = \frac{\langle \psi^I | |\hat{\mu}| | \psi^I \rangle}{\mu_N \sqrt{I(I+1)}}. \quad (6)$$

In the  $g$ -factor calculation, we use the standard values for  $g_l$  and  $g_s$ , namely, the free values for  $g_l$  and the free values damped by a 0.75 factor for  $g_s$ . In Eqs. (5) and (6), wave functions  $|\psi^I\rangle$  are those of Eq. (1).

Presented in the upper part of Fig. 3 are two sets of B(E2) values, calculated at the prolate and oblate minima. It can be seen that the values at the oblate minimum are clearly predicted to be smaller than those at the prolate minimum for the spin states  $I \leq 6$ . A drastic drop of the oblate B(E2) occurs at  $I = 8$ , due to the sharp band crossing of the low- $K$   $i_{13/2}$  neutrons. Thus we predict very different B(E2) values (and hence also quadrupole moments) for the prolate and oblate structures. Similar conclusions can be drawn for  $g$  factors. As the lower part of Fig. 3 shows, there are significant differences between the prolate and oblate  $g$  factors. They both show a drop at  $I = 6$  and 8, due to the rotation alignment of neutrons; however a much greater drop occurs for the oblate  $g$  factors, which even causes the sign to change. Experimental observation of the differences in electromagnetic properties will definitely determine the structure around the crossing point, and thus provide a crucial test for our prediction. We note that new experimental information may soon be available [26].

In conclusion, by using the Projected Shell Model, which conserves total angular momentum and includes configuration mixing beyond the usual mean-field, we have demonstrated a new type of shape phase transition that occurs along the yrast cascade in  $^{190}\text{W}$ . The transition is driven by the dynamic process of rotation alignment of the high- $j$  neutrons, which leads to the preferred state suddenly changing shape from prolate to oblate at  $I = 10$ . The transition results in oblate shape isomers, extending the predictions of Ref. [10]. We have proposed testable quantities for future experiments to measure. Finally, we note that our searching for energy minima has been restricted to axial symmetry. A more general case will be minimization in the  $\varepsilon$ - $\gamma$  plane with three-dimensional angular momentum projection. This is the subject of future work.

This work was supported in part by the U.S. NSF through grant PHY-0216783, the UK EPSRC and AWE plc., the NNSF of China under contract Nos. 10425521, 10475002, 10525520, 10575004, 10675007, the Key Grant Project of Chinese Ministry of Education (CMOE) under contract No. 305001, the Research Fund for the Doctoral Program of Higher Education of China through



grant 20040001010, and by the Chinese Major State Basic Research Development Program through grant 2007CB815005.

## References

- [1] R. F. Casten, *Nature Phys.* **2** (2006) 811.
- [2] F. Iachello, N. V. Zamfir, and R. F. Casten, *Phys. Rev. Lett.* **81** (1998) 1191.
- [3] F. Iachello and N. V. Zamfir, *Phys. Rev. Lett.* **92** (2004) 212501.
- [4] R. F. Casten, D. Kusnezov, and N. V. Zamfir, *Phys. Rev. Lett.* **82** (1999) 5000.
- [5] P. H. Regan, *et al.*, *Phys. Rev. Lett.* **90** (2003) 152502.
- [6] P. Cejnar and J. Jolie, *Phys. Rev. C* **69** (2004) 011301(R).
- [7] Y.-X. Liu, L.-Z. Mu, and H. Wei, *Phys. Lett. B* **633** (2006) 49.
- [8] F.-R. Xu, P. M. Walker, and R. Wyss, *Phys. Rev. C* **62** (2000) 014301.
- [9] P. Stevenson, *et al.*, *Phys. Rev. C* **72** (2005) 047303.
- [10] P. M. Walker and F.-R. Xu, *Phys. Lett. B* **635** (2006) 286.
- [11] R. R. Hilton and H.-J. Mang, *Phys. Rev. Lett.* **43** (1979) 1979.
- [12] P. M. Walker and G. D. Dracoulis, *Nature* **399** (1999) 35.
- [13] Zs. Podolyák, *et al.*, *Phys. Lett. B* **491** (2000) 225.
- [14] A. Frank, P. Van Isacker, and F. Iachello, *Phys. Rev. C* **73** (2006) 061302(R).
- [15] R. Fossion, D. Bonatsos, and G. A. Lalazissis, *Phys. Rev. C* **73** (2006) 044310.
- [16] Y. Alhassid, S. Levit, and J. Zingman, *Phys. Rev. Lett.* **57** (1986) 539.
- [17] P. Federman, S. Pittel, and R. Campos, *Phys. Lett. B* **82** (1979) 9.
- [18] N. Shimizu, T. Otsuka, T. Mizusaki, and M. Homma, *Phys. Rev. Lett.* **86** (2001) 1171.
- [19] M. Hasegawa, K. Kaneko, T. Mizusaki, and Y. Sun, *Phys. Lett. B* **656** (2007) 51.
- [20] K. Hara and Y. Sun, *Int. J. Mod. Phys. E* **4** (1995) 637.
- [21] Y. Sun, J.-y. Zhang, and M. Guidry, *Phys. Rev. Lett.* **78** (1997) 2321.
- [22] R.-D. Herzberg, *et al.*, *Nature* **442** (2006) 896.
- [23] T. Bengtsson and I. Ragnarsson, *Nucl. Phys. A* **436** (1985) 14.
- [24] R. V. F. Janssens *et al.*, *Phys. Lett. B* **131** (1983) 35.
- [25] E. Bouchez *et al.*, *Phys. Rev. Lett.* **90** (2003) 082502.
- [26] P. H. Regan, private communication.